Controlling chaotic scattering: Impulsively driven Morse potential

Zi-Min Lu, Michel Vallières, and Jian-Min Yuan
Department of Physics and Atmospheric Science, Drexel University, Philadelphia, Pennsylvania 19104-9984

James F. Heagy
Naval Surface Warfare Center, 10901 New Hampshire Avenue, Silver Spring, Maryland 20903-5000
(Received 3 June 1991)

We investigate classical chaotic scattering between two atoms interacting via a Morse potential in the presence of a laser field. We find that stable resonance islands appear in phase space above the field-free dissociation energy in an impulsively driven model. A local expansion relating this model to the Hénon map predicts the existence of such resonance islands within some finite domain in parameter space for any similar impulsively driven potential model. By switching on the external field during the collision we show how stable field-dressed molecules can be formed with energy above the field-free dissociation threshold. The experimental and quantum relevance of such phenomenon is discussed.
PACS number(s): 05.45+b

I. INTRODUCTION

This paper is the first in a series of two papers [1] describing the process of atomic collisions in the presence of a laser field which exhibit chaotic scattering and which, at the same time, can be controlled. The chaotic scattering occurs as a result of stable structures in phase space, whose energy lies above the field-free dissociation energy. This novel property suggests a control mechanism by which to trap the system within the field-free continuum. This is carried out by switching on the laser during the collision, creating a stable resonance island within the continuum. We refer to this process as *controlled chaotic scattering*. This control mechanism would be relevant to the process of stimulated molecular recombination.

Chaotic scattering [2–4] and the control of chaos [5] have recently become exciting research areas. Recent studies in chaotic scattering have delineated the roles played by chaotic repellers and homoclinic tangling in this type of transient chaos. Several routes to chaotic scattering have been presented in the literature. Most of our understanding of chaotic scattering is derived from studying time-independent two-(or higher-) degree-of-freedom systems, often with purely repulsive potentials. For potential systems with coexisting bound and continuum spectra we might expect different mechanisms and routes to chaos [4]. We show in this paper that for two atoms interacting via a Morse potential bound-state-like structures are generated in the field-free continuum in the presence of an external electromagnetic field [6]. We also show how these structures influence the scattering process between these two atoms.

Collisions between atoms with subsequent photon emission is an important process for the formation of molecules in the interstellar medium. The probability of such a radiative association process is usually very small, except at extremely low temperature [7]. On the other hand, controlling chemical reactions by using a laser field of arbitrary amplitude, frequency, and pulse shape is an actively pursued area of research [8]. In particular, it would be very interesting if one could enhance the molecular association rate by employing an external field. It would be even more interesting if one could stabilize a pair of atoms with the total energy above the field-free dissociation energy, by irradiating the collision region with an external laser field. To this end the second purpose of this paper is to show how this can be achieved within the context of a simple classical model. These processes, if experimentally feasible, could also find applications in enhancing chemical reactivity by forming highly energetic field-dressed molecules. Unfortunately, as will be discussed below, the required field strength for the controlling mechanism proposed here seems very high.

The Morse oscillator has been extensively used as a model for many physical processes, including infrared multiphoton excitation, dissociation, and overtone absorption of diatomic molecules [9–25]. In all of these studies bound initial states were involved. In this paper we are focusing strictly on collisional processes, emphasizing the unbound motion. Chemical reactions influenced by an external laser field were studied since the mid 1970s; atom-atom collisions [26, 27] and atom-diatom reactions were studied [28–30], as well as larger systems [31]. Most of these studies involved field-induced electronic transitions between two or more states, with the exception of Orel and Miller [29], who treated infrared enhancement of chemical reactions using a single electronic state and a dynamical treatment of the field variables as classical harmonic oscillators. We restrict ourselves in this paper to processes involving only a single electronic state and emphasize the occurrence of chaotic scattering due to invariant phase-space structures.

This first paper in a series of two treats the electromag-

netic laser field as a series of δ-function impulses. The advantage is that the resulting Poincaré map is piecewise analytic and easily implemented, allowing a more intuitive understanding of the chaotic scattering and its control with minimal computational expense. The second paper in the series will treat the continuously driven model, which is more closely related to the experimental situation.

Following this introduction, in the following section we describe the model and the methods of solution. In Sec. III the bound-state-like structures found in the field-free Morse continuum are discussed. Section IV contains an approximation of the scattering Morse map in the vicinity of the minimum of the forcing function by a quadratic (Hénon) map. In Sec. V we show how resonance islands within the continuum influence the scattering process. The control mechanism that we propose to form *field-dressed molecules* as well as normal molecules is discussed in Sec. VI. Section VII deals with our choice of the dipole function. We conclude in Sec. VIII.

II. MODEL AND SOLUTION

The Hamiltonian describing the collision of two nonidentical atoms under the influence of an external laser field consists of two parts: an interaction Hamiltonian between the two atoms and an interaction term between the atoms and the external field,

$$H = H_0 + H_{\rm int}. \tag{1}$$

We consider in this paper the interplay between the external field and the relative motion (or vibrational) degree of freedom of the diatomic system; we assume a decoupling from the orbital (or rotational) motion. We use the time-honored Morse potential to describe the relative motion, namely

$$H_0 = \frac{p^2}{2} + \frac{1}{2}\left(1 - e^{-x}\right)^2. \tag{2}$$

Here all variables are dimensionless as defined in Ref. [9] and the form of the Morse potential is *universal*, its depth and range having been scaled away. The dissociation energy is 0.5 in these units. Within the dipole approximation the interaction Hamiltonian consists of an infinite series of one-sided δ functions and can be written as

$$H_{\rm int} = -A\mu(x) \sum_{n=-\infty}^{n=+\infty} \delta(\tau - nT), \tag{3}$$

where $\mu(x)$ is the dipole moment of the diatomic system and τ is the scaled time. The field is characterized by its scaled strength A and period $T = \frac{2\pi}{\Omega}$. It is assumed that the electric field is linearly polarized along axis of the diatomic system. The dipole moment of the molecule takes the realistic form [32]

$$\mu(x) = (x + a)e^{-(x+a)/b}, \tag{4}$$

where a and b are related to the zero and the width of μ. These parameters will be taken as a=b=2 (in dimensionless units) in most of what follows; $\mu(x)$ then peaks at the Morse potential equilibrium distance (x=0). We will study the case $a \neq b$ in Sec. VIII.

From a practical point of view, a great advantage of the interaction Hamiltonian (3) is that it transforms Hamilton's equations explicitly into a stroboscopic map synchronized with the external field period T. There is a natural simplicity in using this externally synchronized map instead of using a map based on some frequency of the Morse oscillator [33]. In this map the dynamical variables can be taken either as (x,p) or the energy and an extended angle variable (E,θ). If we synchronize the map on the time just prior to the impulse, the map M is naturally decomposed into an impulse K, followed by a free evolution F under the Morse potential for one period T of the external field, namely

$$\begin{pmatrix} x_{n+1} \\ p_{n+1} \end{pmatrix} = M \begin{pmatrix} x_n \\ p_n \end{pmatrix}, \quad M = F \circ K. \tag{5}$$

This map is piecewise analytic. The first term, the kicking term K, is obtained by solving Hamilton's equations from just before the kick to just after the kick; it changes the momentum impulsively and keeps x fixed,

$$\begin{pmatrix} x_n' \\ p_n' \end{pmatrix} \equiv K \begin{pmatrix} x_n \\ p_n \end{pmatrix} = \begin{pmatrix} x_n \\ p_n - A\frac{x_n}{a}e^{-(x_n+a)/a} \end{pmatrix}. \tag{6}$$

The free-evolution term F propagates the trajectory for a period T ahead along the constant energy E curve,

$$\begin{pmatrix} E \\ \theta + \omega T \end{pmatrix} = F \begin{pmatrix} E \\ \theta \end{pmatrix}, \tag{7}$$

where $\omega = \omega(E)$ is the frequency of the Morse oscillator.

The free trajectory is obtained by integrating dx/p from energy conservation

$$\tau(x,p) - \tau(x_{\rm min}, p = 0) = {\rm sgn}(p) \int_{x_{\rm min}}^{x} \frac{dx}{\sqrt{2E - (1 - e^{-x})^2}}, \tag{8}$$

where E is the total energy and sgn(p) takes the values $+1$ or -1 for p positive or negative. If the time origin is chosen at $x_{\rm min} = -\ln(1 + \sqrt{2E})$, then the time parameter has the following symmetry under time reversal: $\tau(x,p) = -\tau(x,-p)$. The integral has two different regimes depending on whether the system is bound ($E \leq 0.5$) or unbound. For the bound case, integrating Eq. (8), and solving for x we obtain

$$x(E,\theta) = \ln\left(\frac{1 - \sqrt{2E}\cos\theta}{\omega^2}\right), \tag{9}$$

where the angle variable

$$\theta = \omega\tau(x,p) \tag{10}$$

parametrizes the position on the trajectory and

$$\omega = \sqrt{1 - 2E} \tag{11}$$

is the Morse frequency. The momentum is

$$p(E,\theta) = \frac{\omega\sqrt{2E}\sin\theta}{1-\sqrt{2E}\cos\theta}. \tag{12}$$

For the unbound case if we define $\tilde{\omega}$ as

$$\tilde{\omega} = \sqrt{2E-1}, \tag{13}$$

and follow the same procedure we obtain

$$x(E,\eta) = \ln\left(\frac{-1+\sqrt{2E}\cosh\eta}{\tilde{\omega}^2}\right), \tag{14}$$

$$p(E,\eta) = \frac{\tilde{\omega}\sqrt{2E}\sinh\eta}{-1+\sqrt{2E}\cosh\eta}, \tag{15}$$

with the extended angle variable η defined as

$$\eta = \tilde{\omega}\tau(x,p). \tag{16}$$

In this case the variable η spans the range $-\infty \leq \eta \leq \infty$. Equations (14) and (15) can be obtained by analytic continuation from Eqs. (9) and (12), namely, by applying the following substitution: $\theta \rightarrow i\eta$ and $\omega \rightarrow i\tilde{\omega}$.

The algorithm for the time evolution through one period of the external field proceeds according to the following steps: (i) From a given point (x,p) on a free trajectory, apply K, i.e., Eq. (6); this is illustrated in Fig. 1(a). (ii) Compute the energy E_{n+1} knowing x_n and p'_n,

$$E_{n+1} = \frac{p'^2_n}{2} + \frac{1}{2}\left(1-e^{-x'_n}\right)^2. \tag{17}$$

This allows us to decide on the form of the subsequent free evolution. (iii) Find the corresponding angle variable for the given x and new p values: if $E_{n+1} < 0.5$, then θ'_n is determined by

$$\cos\theta'_n = \frac{1-e^{x_n}(1-2E_{n+1})}{\sqrt{2E_{n+1}}}, \tag{18}$$

$$\sin\theta'_n = \frac{p'_n e^{x_n}\sqrt{(1-2E_{n+1})}}{\sqrt{2E_{n+1}}}; \tag{19}$$

if $E_{n+1} > 0.5$, then η'_n is determined by

$$\cosh\eta'_n = \frac{1+e^{x_n}(2E_{n+1}-1)}{\sqrt{2E_{n+1}}}, \tag{20}$$

$$\sinh\eta'_n = \frac{p'_n e^{x_n}\sqrt{(2E_{n+1}-1)}}{\sqrt{2E_{n+1}}}, \tag{21}$$

as illustrated in Figs. 1(b) and 1(c). (iv) Apply the free evolution part of the map for either bound or unbound motion. For bound motion we obtain

$$x_{n+1} = \ln\left(\frac{1-\sqrt{2E_{n+1}}\cos(\theta'_n+\omega_{n+1}T)}{1-2E_{n+1}}\right), \tag{22}$$

$$p_{n+1} = \frac{\sqrt{2E_{n+1}(1-2E_{n+1})}\sin(\theta'_n+\omega_{n+1}T)}{1-\sqrt{2E_{n+1}}\cos(\theta'_n+\omega_{n+1}T)}. \tag{23}$$

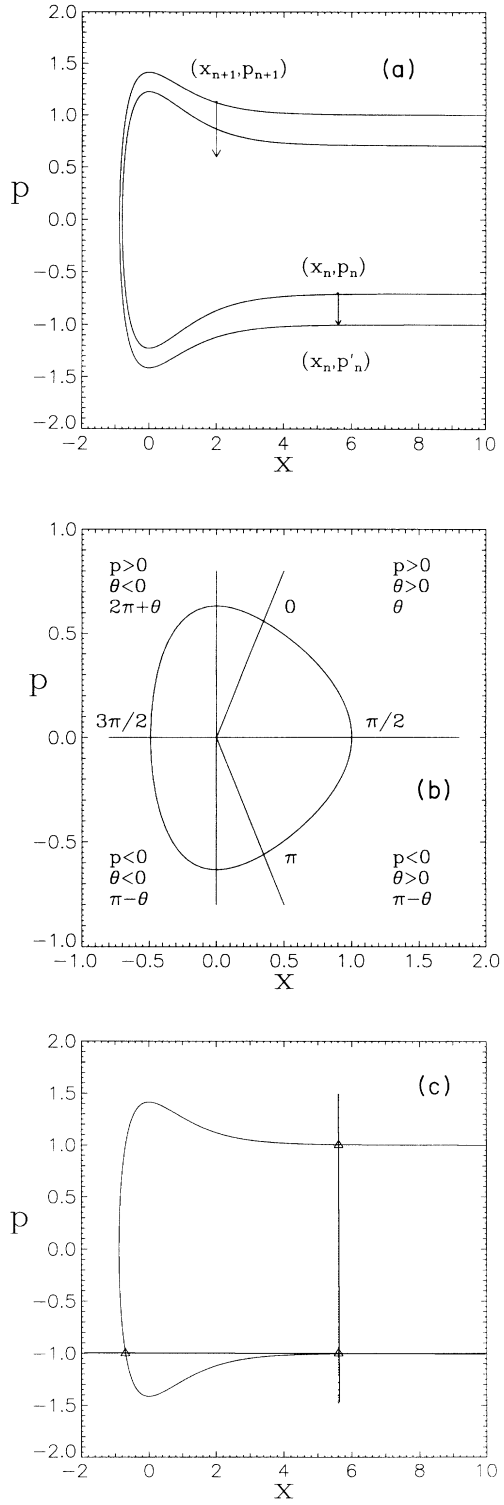

FIG. 1. (a) Impulsively driven part of the map K produces a transition to a free propagation (bound or unbound) with an energy that can be easily evaluated knowing x and p. (b) The choice of θ such as to make Eqs. (9)–(12) consistent when solving for θ, given x and p values. (c) The angle η corresponding to a given phase-space location (x,p) is found for the free unbound case by inverting Eq. (14) for the given $x(E,\eta)$ and Eq. (15) for the given $p(E,\eta)$ and keeping the overlapping solution.

For unbound motion

$$x_{n+1} = \ln\left(\frac{-1+\sqrt{2E_{n+1}}\cosh(\eta'_n+\tilde{\omega}_{n+1}T)}{2E_{n+1}-1}\right), \quad (24)$$

$$p_{n+1} = \frac{\sqrt{2E_{n+1}(2E_{n+1}-1)}\sinh(\eta'_n+\tilde{\omega}_{n+1}T)}{-1+\sqrt{2E_{n+1}}\cosh(\eta'_n+\tilde{\omega}_{n+1}T)}. \quad (25)$$

Therefore the map can be expressed analytically.

III. STRUCTURES IN THE FIELD-FREE CONTINUUM

Based on the analysis of conservative scattering systems, where *unstable* periodic orbits play important roles in determining the scattering behavior [4, 34], we set out in this section to find periodic orbits in phase space. In particular we look for structures in the field-free continuum since one of the aims of this work is to demonstrate the feasibility of stabilizing *field-dressed molecules*, i.e., molecules with energy greater than the dissociation threshold.

In the absence of an external field ($A = 0$) the trajectory E=0.5 constitutes a separatrix which demarcates clearly the closed invariant curves of the bound trajectories from the unbound ones. The latter describe atomic collisional trajectories with $E \geq 0.5$, which can never bind, the energy being conserved. With the field turned on this picture changes drastically. A previous classical study [9] revealed the very complicated dependence of phase-space structures as functions of A and T in the bound region. It was shown classically that dissociation occurs following the breakup of Kolmogorov-Arnold-Moser (KAM) curves, allowing trajectories to escape to the region with $E > 0.5$ [22, 35].

We now set out to find structures in the field-free continuum. The orbits symmetric in p of low periodicity are easily found by a numerical one-dimensional search. These orbits require at least one impulse to take the trajectory from a point in phase space with momentum $+p$ to a point with $-p$ at some given x. This allows a relation between p and A through the kicking part K of the map. In this case a more general approach based on the symmetry properties of M can be used to locate a large class of periodic orbits known as symmetry periodic orbits [36]. Such an approach was applied to a bound case in Ref. [9] and we generalize it here to unbound case. The approach hinges on the invariance of the Hamiltonian under $p \to -p$. Because of this symmetry the identity can be written as

$$\mathcal{I} \equiv FRFR, \quad (26)$$

where R reverses the momentum, $R(x,p) \equiv (x,-p)$. Therefore $F = RF^{-1}R$ and the map can be written as

$$M = RF^{-1}RK \equiv I_1 I_0, \quad (27)$$

where $I_1 = RF^{-1}$ and $I_0 = RK$. These operators satisfy the relations $I_1^2 = I_0^2 = \mathcal{I}$ and $\det DI_1 = \det DI_0 = -1$, where D is the differential operator. They are known as orientation reversing involutions. The factorization (27) signals the *reversibility* of the map M.

The fixed sets of I_0 and I_1 are known as fundamental symmetry lines. Symmetry lines organize the periodic orbits in reversible maps. Let Γ_0 and Γ_1 be the fixed sets of I_0 and I_1, respectively. Γ_0 is easily obtained from the map K; it takes the form

$$\Gamma_0 = \left((x,p) \;\middle|\; p = -\frac{A}{2}\frac{d\mu}{dx}\right). \quad (28)$$

The symmetry line Γ_1 takes on two components, depending on whether the free evolution F takes place in the bounded or unbounded region. For bounded motion [9] the analytical description of Γ_1 has two branches in (E,θ) representation, depending on the relation of the angle θ to the principal branch of $\cos^{-1}$. They are given by

$$\Gamma_{1,0} = \left((E,\theta) \;\middle|\; \theta = \omega(E)\frac{T}{2}\right), \quad (29)$$

$$\Gamma_{1,1} = \left((E,\theta) \;\middle|\; \theta = \pi + \omega(E)\frac{T}{2}\right). \quad (30)$$

These branches join smoothly at the origin in (x,p) representation. For unbounded motion we must use the free evolution F for $E > 0.5$, which requires the scattering solution Eqs. (14) and (15). This gives

$$\Gamma_1^u = \left((E,\eta) \;\middle|\; \eta = \tilde{\omega}(E)\frac{T}{2}\right), \quad (31)$$

where the superscript u denotes unbound. Γ_1^u has only one branch since the variable η is not subject to the mod2π condition ($-\infty < \eta < \infty$). The maximal invariant set of I_1 is given by the union of the bound and unbound components $\Gamma_1 = \Gamma_{1,0} \cup \Gamma_{1,1} \cup \Gamma_1^u$.

Note that the intersection of Γ_1 with Γ_0 must be a period-1 orbit since $M = I_1 I_0$. Higher-order symmetry lines can be defined to provide the locations of longer periodic orbits. These higher-order symmetry lines can be obtained through iterations of the fundamental symmetry lines Γ_0 and Γ_1 according to

$$\Gamma_{2n} = M^n \Gamma_0, \quad (32)$$

$$\Gamma_{2n+1} = M^n \Gamma_1 \quad (33)$$

(cf. [9, 36]). Care must be taken in constructing Γ_{2n+1} since Γ_1 contains two branches in the bounded region. In general the intersection of any two symmetry lines yields a periodic orbit according to

$$\Gamma_i \cap \Gamma_j \subset \mathcal{P}_{i-j} \quad (34)$$

[36], where $\mathcal{P}_{i-j}$ denotes the set of periodic orbits whose periods divide $|i-j|$. This relation provides an easy way to locate periodic orbits. Figure 2 shows the symmetry lines Γ_0 through Γ_2 for parameters $A = 2e^2$ and $T = 5.271\,719$. Note especially the intersection of Γ_1 with Γ_0 as well as intersections of higher-order symmetry lines with Γ_0; the intersection is a period-1 orbit. This period-1 orbit plays a major role in the scattering process, as discussed below.

Two structures influence strongly the scattering be-

havior, as we will demonstrate below: first the stable period-1 orbit with an energy *greater* than the dissociation energy (0.5) of the Morse potential and the second unstable period-1 orbit in the bound energy region. In the stroboscopic representation, in which the coordinates (x,p) are recorded right before each kick, the location of the period-1 stable orbit is exactly at (2,1), with E=0.873 823 for a kicking amplitude $A=2e^2$ [which follows from $p' - p = -2 = A\mu'(x = 2)$] and period T=5.271 719, respectively. The unstable period-1 orbit is found at $(x,p) = (-0.189\,233, -0.282\,735)$; this orbit is surrounded by a stable period-2 orbit and results from a period-doubling bifurcation which took place at a smaller value of A. The stable period-1 fixed point orbit is surrounded by KAM curves as shown in Fig. 2(b). The shapes of these KAM curves are influenced by a period-3 saddle whose manifolds delineate a stable resonance island of triangular shape [37]. Figure 2(c) shows the location of the period-1 and -3 orbits coinciding with the intersections of symmetry lines.

The organization of the phase space of the Morse continuum changes drastically as the parameters of the field are changed. In particular, the resonance island can change shape and size and even bifurcate with changing field parameters, A or T. Figure 3 shows the change in shape and size along with the period-doubling bifurcation of the island as A changes. Figure 4 shows the first and second bifurcations of the island as T changes. We have superposed the symmetry lines onto the latter figure to show more vividly the organization of these structures.

IV. LOCAL APPROXIMATION BY HÉNON MAP

It is natural to ask to what extent the stable period-1 orbit and associated resonance island within the continuum depend on the choice of dipole function and poten-

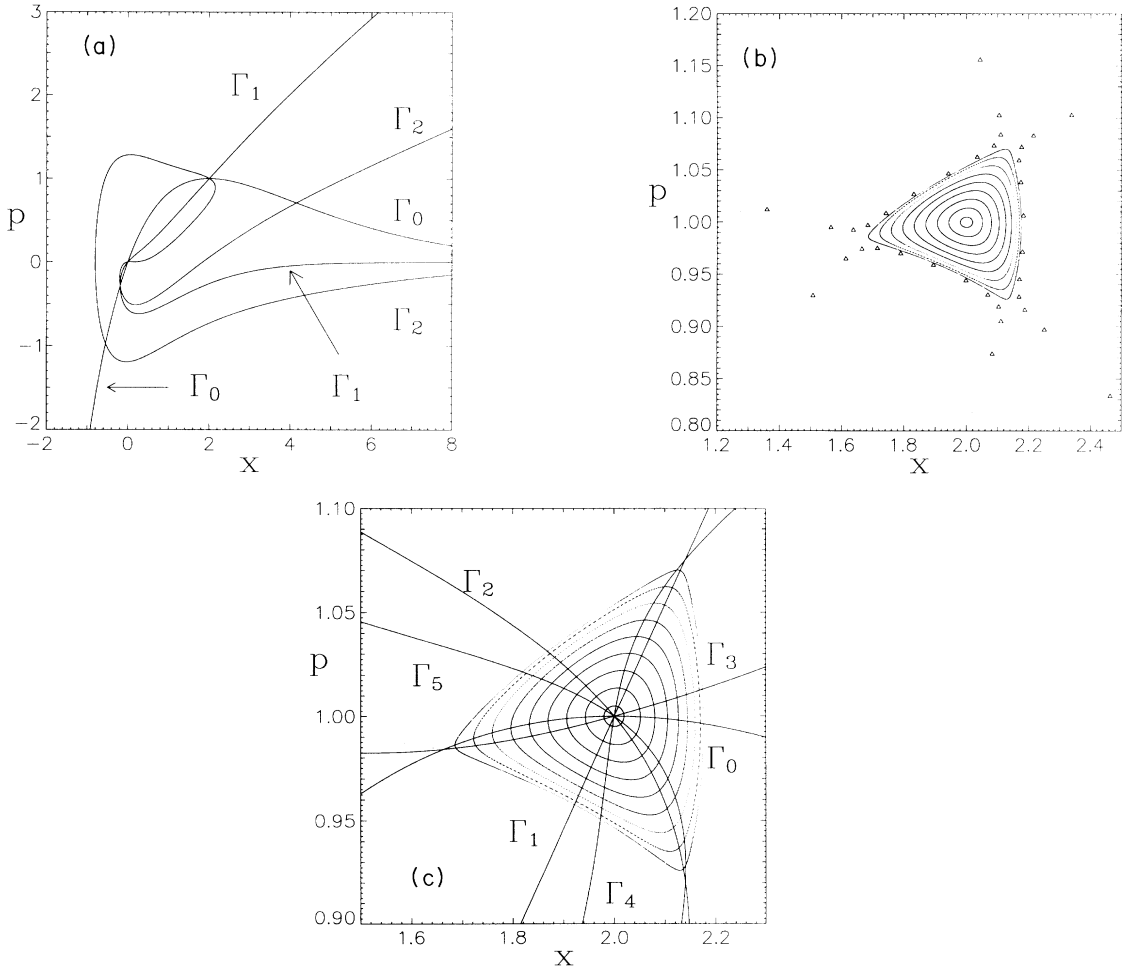

FIG. 2. (a) Symmetry lines Γ_0 to Γ_2 in phase space. Each intersection of two symmetry lines Γ_i and Γ_j indicates a periodic orbit. The amplitude and period of the fields are, respectively, $A=2e^2$ and T=5.271 719. (b) Stroboscopic map (in which x and p are recorded prior to each impulse) showing the KAM curves forming a resonance island in the vicinity of the period-1 orbit located at (x,p)=(2,1) . The energy is 0.873 823 and the field parameters are $A=2e^2$ and T=5.271 719. The period-3 saddle borders the boundaries of the triangular stable resonance region. The dots are computed by multiple iterations of the map for an ensemble of initial conditions near the period-1 orbit. The triangles are points in a stroboscopic map of a particular scattering trajectory shown in Fig. 9(a). (c) Superposition of the symmetry lines onto the resonance island shown in (b).

tial; i.e., do they survive under small change of either? Here we address this question by noting that the stable period-1 orbit is located near the minimum of the dipole coupling force $\mu'(x)$. For a different choice of dipole function we expect this also to be the case. From (4) we have

$$\mu'(x) = -\frac{x}{a}e^{-(x+a)/a}, \tag{35}$$

which has a minimum at $x=a$. In the vicinity of the minimum we can expand $\mu'(x)$ through second-order terms to obtain

$$\mu'(x) = \mu'(a) + \frac{1}{2}\mu'''(a)(x-a)^2, \tag{36}$$

where $\mu'(a) = -e^{-2}$ and $\mu'''(a) = (ae)^{-2}$. The impulsive step K can therefore be approximated by $\mathcal{K}$, defined by

$$\begin{pmatrix} x_n' \\ p_n' \end{pmatrix} \cong \mathcal{K}\begin{pmatrix} x_n \\ p_n \end{pmatrix} = \begin{pmatrix} x_n \\ p_n + A\mu'(a) + \dfrac{A}{2}\mu'''(a)(x_n-a)^2 \end{pmatrix}. \tag{37}$$

The combined approximate map $F\circ\mathcal{K}$ produces results in close resemblance to the original map M, as shown in Fig. 5(a) [compare to Fig. 2(b)]. Note that the unstable period-3 saddle surrounding the period-1 island is also present in $F \circ \mathcal{K}$. In addition, we have also observed the 1:3 resonant bifurcation in $F \circ \mathcal{K}$ that occurs in the original scattering Morse map [cf. Fig. 3(a)].

We now consider the effect of changing the potential. This change reflects itself in the free propagation step F. In general F induces an energy-dependent phase change $\Delta\eta$. Here we approximate this change by a *rigid* rotation of the phase-space coordinates (x_n', p_n') through an angle ψ

$$F \approx \mathcal{R} = \begin{pmatrix} \cos\psi & \sin\psi \\ -\sin\psi & \cos\psi \end{pmatrix}. \tag{38}$$

This yields the approximate map $\mathcal{R} \circ \mathcal{K}$ given by

$$\begin{pmatrix} x_{n+1} \\ p_{n+1} \end{pmatrix} = \begin{pmatrix} \cos\psi & \sin\psi \\ -\sin\psi & \cos\psi \end{pmatrix} \times \begin{pmatrix} x_n \\ p_n + A\mu'(a) + \dfrac{A}{2}\mu'''(a)(x_n-a)^2 \end{pmatrix}. \tag{39}$$

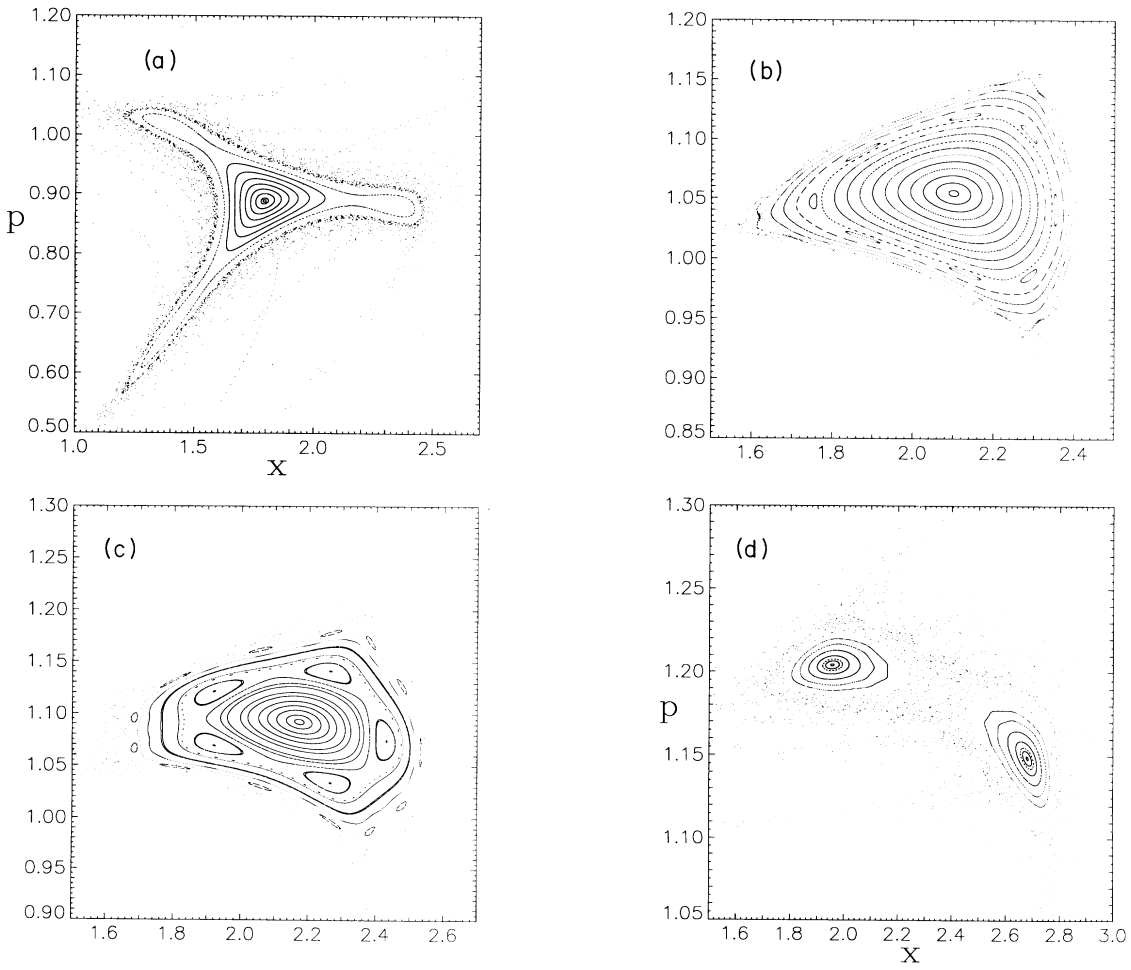

FIG. 3. Composite figure showing the changes that occur to the resonance island surrounding the period-1 orbit as A is changed while keeping T fixed (T=5.271719). (a) A=13.2. (b) A=15.6. (c) A=16.2. (d) A=17.8.

The rigid rotation approximation (38) places all of the nonlinearity within the kicking step $\mathcal{K}$. In order for (39) to possess a period-1 orbit with $x > 0$ the rotation angle ψ must be greater than π; it is sufficient to consider rotation angles $\pi < \psi < 2\pi$. If the angle is taken to be T itself, the rigid rotation $\mathcal{R}$ is equivalent to approximating the Morse potential with a harmonic oscillator.

We note the similarity of the map (39) to the area-preserving quadratic map introduced by Hénon [38]. It can be shown that (39) can be reduced to a one-parameter quadratic map under a linear transformation of coordinates, and is therefore equivalent to the area-preserving Hénon map (cf., Ref. [39] for a related study).

The map (39) has a stable period-1 orbit (with $x>0$) provided the quantity

$$\rho = -\frac{A}{4}\mu''' \sin\psi \left[\left(\frac{2(\cos\psi - 1)}{a\mu''' \sin\psi}\right)^2 - 2\frac{\mu'}{\mu'''} - a^2\right]^{1/2} \tag{40}$$

satisfies $0 < \rho < 1$ (ρ is the residue of the orbit [40]). Since $A > 0$ and $\sin\psi < 0$ we see that a necessary condition for a stable period-1 orbit is $\mu''' > 0$. This is consistent with our earlier expectation of a stable period-1 orbit near the minimum of $\mu'(x)$. The condition $\mu'''(a) > 0$ is expected to be satisfied for realistic dipole functions; for the dipole function (4) this arises from the exponential falloff of $\mu(x)$ for large x. Figure 5(b) shows several orbits of the map (39) with $\psi = T = 3.8, A = 2e^2, a = 2$, and derivatives μ' and μ''' computed from the dipole function (4). The approximate map displays the same qualitative features as seen in the exact map M, notably the existence of the stable period 1 surrounded by a period-3 saddle (the location of the stable island is not accurately rendered due to the energy-independent rigid rotation approximation of F). These results give us reason to believe that our choices of dipole function and potential are not restrictive, and that other choices should also yield stable period-1 orbits in the continuum for a range of parameters A and T.

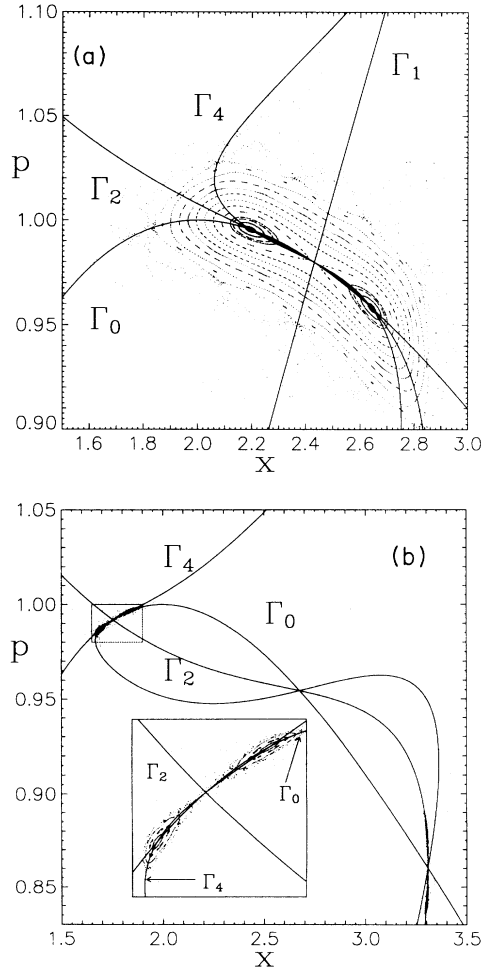

FIG. 4. Composite figure showing the first and second period doubling of the resonance island as T is changed while keeping A fixed ($A=2e^2$). (a) Period-2 orbit resulting from the period doubling of the period 1; T=6.07. (b) Bifurcation of period-2 orbit resulting in a period-4 orbit; T=6.6.

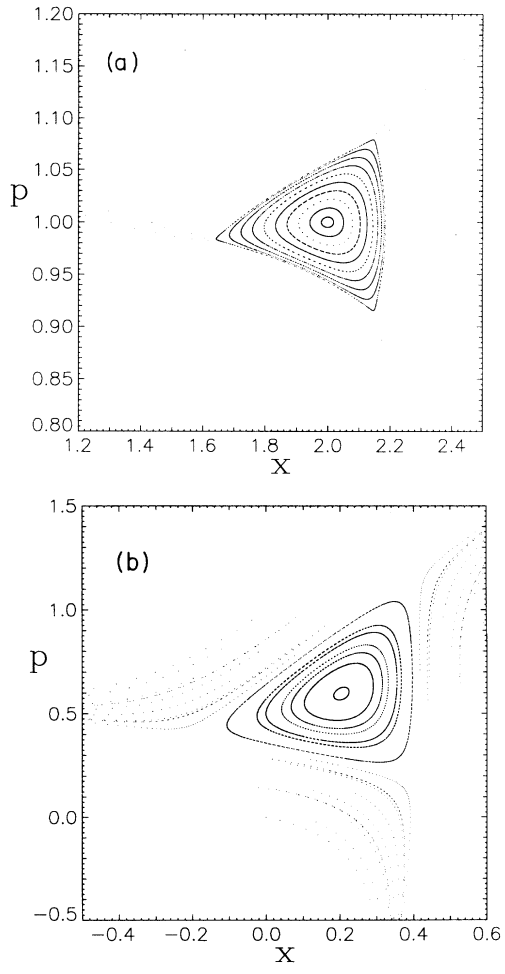

FIG. 5. (a) Period-3 saddle surrounding the period-1 orbit calculated with the approximate map $F \circ \mathcal{K}$ of Eq. (37) for the same parameters as in Fig. 2(b). (b) Same as in (a), but calculated using the map $\mathcal{R} \circ \mathcal{K}$ of Eq. (38), for the same A and for T=3.8.

V. CHAOTIC SCATTERING

The model we treat in this paper has one degree of freedom; therefore the atomic scattering process that it describes depends only on the energy (or momentum) of the incoming atoms in the asymptotic region and on the phase of the electromagnetic field with respect to the phase of the Morse oscillator. The latter is not easily observable in real experimental situations and therefore will be kept fixed (at zero) or averaged over in what follows. An observable that is a characteristic measure of the scattering process in a one-degree-of-freedom space is the collision time; the time for a round-trip from the asymptotic region to the collision region and back to the asymptotic region. Figure 6 shows the collision times associated with 2000 trajectories originating from x=20, where both the Morse potential and dipole function approach their asymptotic values. The initial conditions are equally distributed in momenta in the interval $-2.5 < p < -0.01$ and with the phase set to 0. An expansion of scale in this figure reveals finer structures (multiple peaks separated by smooth regions) over many orders of magnitude. These collision times show the characteristic discontinuity over a fractal set of initial conditions. This is the hallmark of chaotic scattering.

The singularity of the scattering functions (cross section, collision time, etc.) are usually caused by the stable manifolds reaching out into the asymptotic region. The two atoms can stick together for an infinitely long time if the scattered particle moves in along a stable manifold. Chaotic scattering requires that the set of singularities be fractal. To illustrate this point we plot in Fig. 7 the backward iterations of an ensemble of trajectories originating near the period-3 stable manifolds. The intersection of these trajectories with the line of initial conditions, x=20, gives exactly the locations in momenta where the collision time becomes singular. A continuous enlargement of Fig. 6 or 7 over initial conditions reveals a self-similar structure characteristic of Cantor sets. If we come in on the stable manifold of the period-3 saddle *exactly* the τ_c *is* infinite. Of course, τ_c in numerical simulation never actually goes to infinity, but it can be made arbitrarily long. Note that his set is not *hyperbolic* because there are still unbroken KAM curves. The measure of the fractal set appears to be zero (i.e., the gaps have full measure).

Figure 8(a) shows the stroboscopic section of the same trajectories that made up Fig. 6. Figure 8(b) shows the unstable manifolds of the period-3 saddle surrounding the stable island associated with the period-1 orbit; these unstable manifolds organize the scattering pattern.

There are two mechanisms that underlie the longer collision times seen in Fig. 6. The first one occurs when a trajectory approaches the period-3 saddles (surrounding the period-1 island) near the stable manifold of the saddle; this is exemplified in Fig. 9(a). Another possibility results from a trajectory that gets kicked near the free-field separatrix, $E = 0.5$, as the trajectory leaves

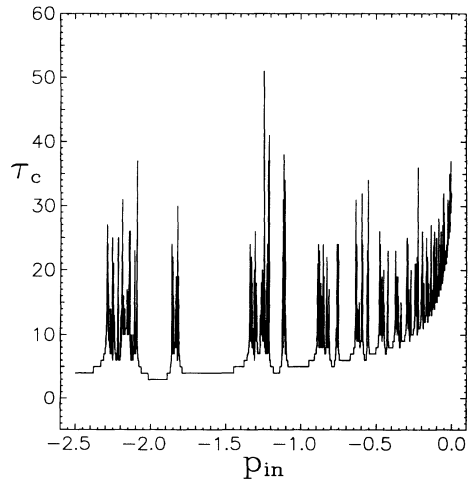

FIG. 6. Collision times of scattering trajectories originating from x=20, with momenta equally distributed in the range $p = (2.5, -0.01)$ and with zero phase for field parameters A=2e^2 and T=5.271 719.

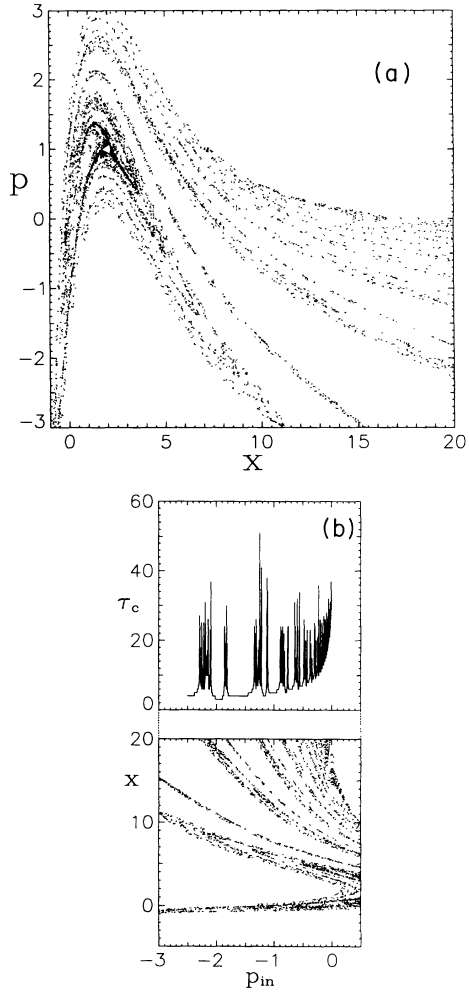

FIG. 7. (a) Backward iterations of an ensemble of trajectories originating near the period-3 stable manifolds. (b) The intersections of the trajectories in (a) with the line x=20 give exactly the locations in momenta where the collision times become large.

the scattering region. Since the kicks get smaller as x increases the orbit can reenter the potential and remain near the separatrix for several iterations of the map. This mechanism is shown in Fig. 9(b). Each case constitutes a *pseudotrapping* mechanism capable of producing *arbitrarily long collision times* .

Figure 2(b) shows the stroboscopic surface of section of the trajectory which generates a long collision time using the mechanism exemplified in Fig. 9(a). Scattering points never penetrate the stable island which now forms a *repeller*. This is complementary to the dissociation process whereby a molecule cannot dissociate through closed KAM curves [9].

VI. CONTROLLING THE CHAOTIC SCATTERING

We see in Sec. IV that a resonance island appears in the field-free continuum as a result of the external field. This suggests that one can stabilize a pair of atoms by using an external field to form a stable field-dressed molecule with energy above the dissociation limit by bringing the system within these stable islands. Since the scattering trajectories cannot penetrate the stability island from outside, a simple scattering process as described in the preceding section is not sufficient to produce such field-dressed molecules. We can overcome this difficulty by switching on or off the external field during collisions; for instance, an experimentalist could use a pulsed laser field or simply allow the atomic beams to pass through a region permeated by a confined laser beam. We consider a sudden switching-on of the external field in the atomic collision region. The phase between the external field and the Morse oscillator can not be fixed experimentally; we simulate the effect of this extra parameter by using different initial x values in a small interval in the asymptotic region corresponding to a $[-\pi,\pi]$ interval in phase centered on a nominal x value having zero phase at the center of the stable island. Figure 10 shows the collision times for trajectories initiated at these x val-

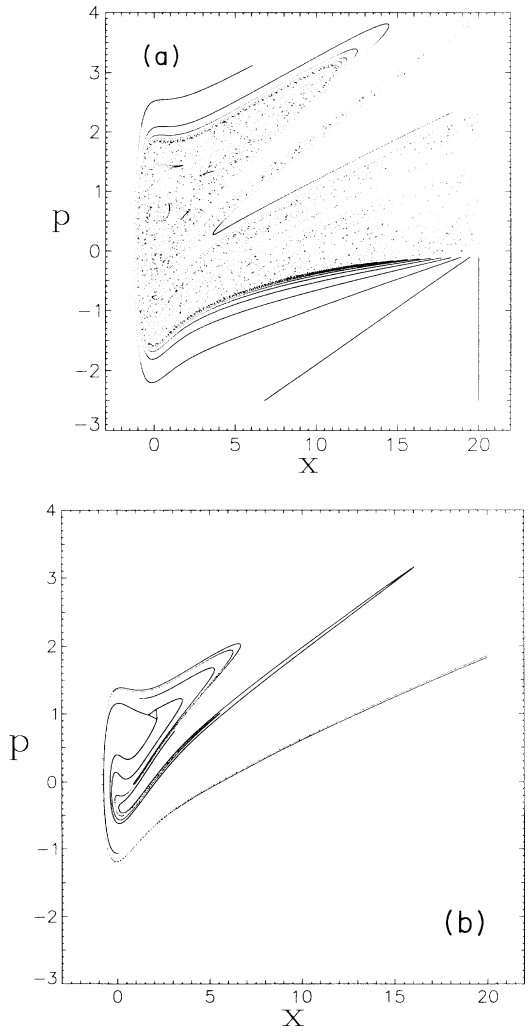

FIG. 8. (a) Stroboscopic map of the scattering trajectories that contribute to collision times in Fig. 6. (b) Unstable manifolds of the period-3 saddle.

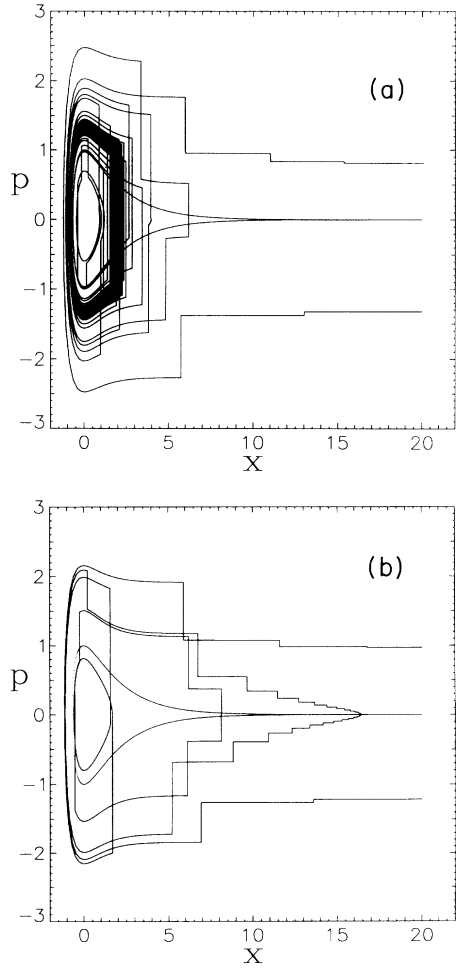

FIG. 9. (a) Particular *trapped* trajectory influenced by the period-1 stable orbit which causes the peak at $p=-1.323\,702$ in Fig. 6. (b) Particular collision trajectory which reaches an energy $E \simeq 0.5$ at large distances which can cause a very long collision time. This orbit causes the peak at $p= -1.213\,750$ in Fig. 6.

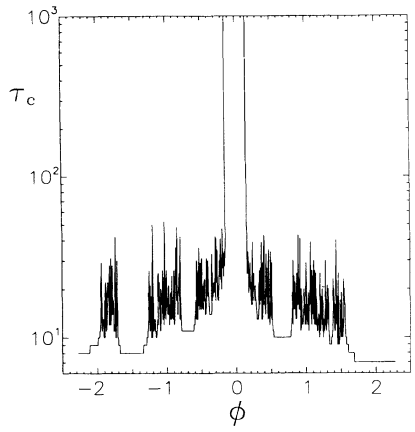

FIG. 10. Collision times of a set of trajectories originating asymptotically with $p_{in} = -0.864\,665$, and x in a small interval centered on x=20.389 025 so as to produce a range in phase of $[-\pi,+\pi]$ with phase zero centered on the fixed point corresponding to the period-1 orbit. The field parameters are $A=2e^2$ and T=5.271 719.

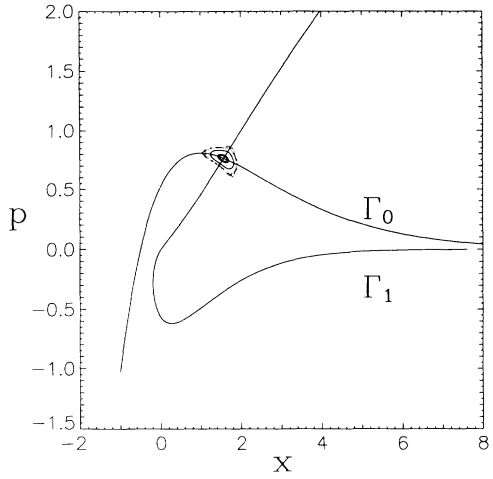

FIG. 11. Intersection of the symmetry lines Γ_0 and Γ_1 giving the location of period-1 fixed point for parameters a=2 and b=1.5, field parameters A=12.0, and T=5.27.

ues. We find that about 6% of the initial conditions are captured within the resonance island. We conclude that *stable field-dressed molecules can be formed in the field-free continuum of the Morse potential* by this process.

The formation of a *bound state* of the molecule in the Morse continuum is a nontrivial result. It suggests the possibility of forming a field-dressed molecule. It is anticipated that the field-dressed molecule could have enhanced reactivity as compared to the normal molecule because of its extra energy content.

The mechanism for the formation of a field-dressed molecule that we propose requires the existence of a stable island in the field free continuum. As we have seen the stable island is a prerequisite to chaotic scattering. Therefore we propose to control chaotic scattering by guiding the system toward the stable islands. Ott, Grebogi, and Yorke [5] have proposed recently a control mechanism for chaotic systems in which the previous knowledge of the dependence of the local manifolds of a saddle point on a system parameter is used to continuously adjust the system toward the stable manifold. The control mechanism proposed here for chaotic scattering is quite different.

Controlling chemical reactions by using a laser field of arbitrary amplitude, frequency, and pulse shape is an actively pursued area of research [8]. In particular, it would be very interesting if one could enhance the molecular association rate by employing an external field. In this case, one would like to form real molecules, i.e., molecules in the bound region of the Morse potential after the external field is switched off. This process would require the trapping of scattering trajectories with energy less than the dissociation threshold. A superposition of the dissociation energy separatrix (E=0.5) onto Fig. 9 does show that a significant fraction of the trajectories have excursions in the bound energy region. This suggests that a switching-off of the laser field would leave many trajectories in a bound molecular state.

VII. THE DIPOLE FUNCTION

We have chosen the dipole function to be

$$\mu(x) = (x + a)e^{-(x+a)/b}, \tag{41}$$

with a and b arbitrary range and width parameters. This functional form leads to a good approximation for the dipole functions of many observed molecules [32]. So far we have chosen $a = b = 2$ (dimensionless units) in our discussion. This leads to a particular situation where the origin $(x,p) = (0,0)$ is a fixed point of the map. Relaxing this condition can lead to bifurcations and subsequent disappearance of fixed points. If anything, it could be said that, contrarily, the situation in which $a \neq b$ is simpler since fewer features exist in the unbounded phase space. In particular, as the parameter b decreases from 2, the fixed point originally at the origin collides with the lower energy fixed point in an inverse saddle node (tangent) bifurcation, the two fixed points disappearing beyond the bifurcation. Figure 11 depicts the symmetry lines beyond this bifurcation (b=1.5). Note the absence of more than one intersection between the two symmetry lines. A similar bifurcation occurs as b increases. In this case the fixed point originally at the origin collides with the high energy period-1 orbit, also in an inverse saddle node bifurcation. The first of these bifurcations does not lead to qualitatively different scattering behavior since the scattering is most strongly influenced by the period-3 saddle surrounding the high-energy period 1; this is illustrated in Fig. 12. The second bifurcation does change the nature of the scattering since the high-energy period-1 orbit (thus the period-3 saddle) is gone. In this case the scattering is controlled most strongly by the stable and unstable manifolds of the low-energy period-1 flip saddle.

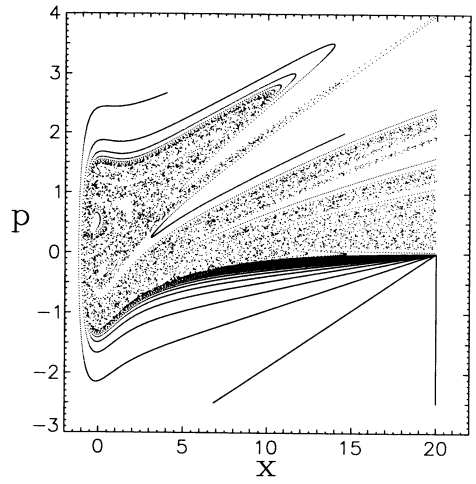

FIG. 12. Poincaré map of the scattering trajectories using the more general dipole function used in Fig. 11.

The local expansion that leads to the quadratic map approximation of the Morse map remains valid in this case. The only difference with Sec. IV above is that the expansion must be carried out at the new minimum, $x = 2b - a$, rather than at $x = a$. This yields different values for the derivatives of the dipole function at the expansion point, namely, $\mu' = -e^{-2}$ and $\mu''' = (be)^{-2}$. Therefore our comments concerning the Hénon map connection and the robustness of the period-1 orbit still apply here.

VIII. DISCUSSIONS AND CONCLUSIONS

We have studied in this paper atomic scattering under the influence of an electromagnetic field with particular emphasis on the physical aspects of field-dressed molecule formation and the connection to chaotic scattering [41, 42]. Our model exhibits chaotic scattering. We have observed the existence of structures in the field-free continuum of the Morse potential induced by the electromagnetic field. We have also shown the connection of the current model map to the Hénon map and illustrated how the period-1 and period-3 orbits that strongly influence the scattering behavior can be directly explained by this quadratic map approximation. We then showed how experiments could be conceived to form field-dressed molecules or to enhance the formation of stable molecules by simply switching on or off the field during the collision process. These methodologies constitute control mechanisms for the chaotic scattering.

The possibility to realize experimentally the ideas proposed in this paper depends on the field strength required. One of the limitations is that the field intensity should not be so high that other processes such as ionization become important. The two aspects of the collisional process treated in this paper, namely chaotic scattering and control, require very different laser intensities. First, we expect the threshold field intensity needed to observe chaotic scattering to be one or two orders of magnitude less than that required to observe multiphoton dissociation of diatomic molecules (about 1 TW/cm^2). This results from the fact that the former process only requires the outer KAM curves to break up, while, on the other hand, the multiphoton dissociation will not commence until the low-energy KAM curves surrounding the potential well have also broken up. It is therefore appealing to think about experiments to show this effect.

The threshold field strength needed to control the scattering via stable features in the continuum must be such as to produce stable features in the continuum. This indeed requires a field of very high intensity. The field strength required is given by

$$E = \frac{\alpha \Omega D A}{q_{\text{eff}}},$$

where q_{eff} is the effective charge, taken as the electronic charge. Assuming a dissociation constant of 1 eV and a range parameter of 1 bohr radius, we calculate that for the parameters used above, one would require roughly 1000 TW/cm^2. These parameters were somewhat arbitrarily chosen and have not been optimized to reduce the field intensity; nevertheless these field strengths might be difficult to realize experimentally. Our hope is that our model illustrates a controlling mechanism which may be useful in some other physical processes and could further stimulate more thoughts on the control problem for microscopic systems.

The model we have used in this paper is simple and allows us much analytical understanding of the atomic scattering problem. In the next paper of this series of two we will use a continuously driven system and illustrate that many of the physical pictures found here carry through to that case.

In principle, stimulated stability of molecules should manifest itself in a quantum-mechanical approach if the size of resonance islands above the field-free separatrix is greater than $\hbar$ (for the Morse potential $\hbar$ is related to the inverse of the number of bound states). The resonance island which surrounds the stable period-1 orbit in Fig. 2(b) has an area $1.5\hbar$ for a system with 24 bound states, appropriate for hydrogen fluoride; in principle this island can therefore support a quantum state. We are currently extending our previous quantum-mechanical treatment of photodissociation [43] to the scattering problem.

ACKNOWLEDGMENTS

We gratefully acknowledge J. E. Bayfield and H. L. Dai for stimulating discussions concerning experimental issues. The work is partially supported by the NSF through Grants Nos. Phy90-04582 and Phy90-06186, and by the donors of the Petroleum Research Funds, administered by the ACS. J.H. is supported by the Office of Naval Technology. We acknowledge Cray supercomputer time from NCSA.

[1] Zi-Min Lu, Michel Vallières, and Jian-Min Yuan (unpublished).
[2] B. Eckhardt and C. Jung, J. Phys. A **19**, L829 (1986); P. Gaspard and S. Rice, J. Chem. Phys. **90**, 2225 (1988).
[3] G. Troll and U. Smilansky, Physica D **35**, 34 (1989); R. Blumel and U. Smilansky, Phys. Rev. Lett. **60**, 477 (1988); Physica D **36**, 111 (1989).
[4] S. Bleher, E. Ott, and C. Grebogi, Phys. Rev. Lett. **63**, 919 (1989); S. Bleher, C. Grebogi, and E. Ott, Physica D **46**, 87 (1990); M. Ding, C. Grebogi, E. Ott, and J. A. Yorke, Phys. Lett. A **153**, 21 (1991).
[5] E. Ott, C. Grebogi, and J. A. Yorke, Phys. Rev. Lett. **64**, 1196 (1990); in *CHAOS: Soviet-American Perspectives on Nonlinear Science*, edited by D. K. Campbell (American Institute of Physics, New York, 1990), p. 153; W. L. Ditto, S. N. Rauseo, and M. L. Spano, Phys. Rev. Lett. **65**, 3211 (1990).
[6] Zi-Min Lu, Michel Vallières, and Jian-Min Yuan (unpublished).
[7] G. H. Dunn, in *Electronic and Atomic Collisions*, edited by D. C. Lorentz, W. E. Meyerhof, and J. R. Peterson (North-Holland, Amsterdam, 1988); L. Frommhold and H. M. Pickett, Chem. Phys. **28**, 441 (1978).
[8] D. G. Imre and J. Zhang, Chem. Phys. **139**, 89 (1989); R. Kosloff, S. A. Rice, P. Gaspard, S. Tersigni, and D. J. Tanner, *ibid.* **139**, 201 (1989); P. Brumer and M. Shapiro, *ibid.* **139**, 221 (1989); A. Hubler and E. Luscher, Naturwissenschaften **76**, 67 (1989); A. Hubler, Helv. Phys. Acta **63**, 343 (1989).
[9] J. F. Heagy and J. M. Yuan, Phys. Rev. A **41**, 571 (1990).
[10] R. B. Walker and R. K. Preston, J. Chem. Phys. **67**, 2017 (1977).
[11] D. W. Noid and J. R. Stine, Chem. Phys. Lett. **65**, 153 (1979).
[12] K. M. Christoffel and J. M. Bowman, J. Phys. Chem. **85**, 2159 (1981).
[13] M. J. Davis and R. E. Wyatt, Chem. Phys. Lett. **86**, 235 (1982).
[14] D. A. Jones and I. C. Percival, J. Phys. B **16**, 2981 (1983).
[15] S. K. Gray, Chem. Phys. **75**, 67 (1983); **83**, 125 (1984).
[16] P. S. Dardi and S. K. Gray, J. Chem. Phys. **80**, 4738 (1984).
[17] R. B. Shirts and T. F. Davis, J. Phys. Chem. **88**, 4665 (1984).
[18] R. M. O. Galvano, L. C. M. Miranda, and J. T. Mendonca, J. Phys. B **17**, L577 (1984).
[19] R. Heather and H. Metieu, J. Chem. Phys. **86**, 5009 (1987); **88**, 5496 (1988).
[20] R. C. Brown and R. E. Wyatt, Phys. Rev. Lett. **57**, 1 (1986); J. Phys. Chem. **90**, 3590 (1986).
[21] D. Poppe and J. Korsch, Physica D **24**, 367 (1987).
[22] Y. Gu and J. M. Yuan, Phys. Rev. A **36**, 3788 (1987).
[23] M. E. Goggin and P. W. Milonni, Phys. Rev. A **37**, 796 (1988); **38**, 5174 (1988).
[24] J. J. Tanner and M. M. Maricq, Phys. Rev. A **40**, 4054 (1989); Chem. Phys. Lett. **14**, 503 (1988).
[25] J. F. Heagy, J. M. Yuan, Z. M. Lu, and M. Vallières, *Dynamics of Driven Molecular Systems*, in *Directions in Chaos*, edited by D. H. Feng and J. M. Yuan (World Scientific, Singapore, 1992), Vol. IV.
[26] N. M. Kroll and K. M. Watson, Phys. Rev. A **13**, 1018 (1976).
[27] Ph. Cahuzac and P. E. Toschek, Phys. Rev. Lett. **40**, 1087 (1978).
[28] J. M. Yuan, T. F. George, and F. J. McLafferty, Chem. Phys. Lett. **40**, 163 (1976); J. M. Yuan and T. F. George, J. Chem. Phys. **68**, 3040 (1978); **70**, 990 (1979); K. Duffy and J. M. Yuan, *ibid.* **88**, 5799 (1984).
[29] A. E. Orel and W. H. Miller, J. Chem. Phys. **70**, 4393 (1979).
[30] A. E. Orel and W. H. Miller, J. Chem. Phys. **73**, 241 (1980); K. C. Kulander and A. E. Orel, *ibid.* **75**, 675 (1981).
[31] P. Hering, P. R. Brooks, R. F. Curl, J. S. Judson, and R. S. Lowe, Phys. Rev. Lett. **44**, 687 (1980).
[32] Gerhard Herzberg, *Molecular Spectra and Molecular Structure I. Spectra of Diatomic Molecules* (Van Nostrand, Toronto, 1950); R. Heather and H. Metiu, J. Chem. Phys. **86**, 5496 (1987); J. F. Ogilvie, W. R. Rodwell, and R. H. Tipping, *ibid.* **73**, 5221 (1980).
[33] R. Graham and M. Höhnerbach, Phys. Rev. Lett. **64**, 637 (1990).
[34] M. Ding, C. Grebogi, E. Ott, and J. A. Yorke, Phys. Rev. A **42**, 7025 (1991).
[35] J. Heagy, Ph.D thesis, Drexel University, 1990 (unpublished).
[36] R. DeVogelaere, in *Contributions to the Theory of Nonlinear Oscillations*, edited by S. Lefschetz (Princeton University Press, Princeton, 1958), Vol. IV, p. 53.
[37] V. I. Arnold, *Mathematical Methods of Classical Mechanics* (Springer-Verlag, New York, 1978); D. K. Arrowsmith amd C. M. Place, *An Introduction to Dynamical Systems* (Cambridge University Press, Cambridge, England, 1990).
[38] M. Hénon, Q. Appl. Math. **27**, 291 (1969).
[39] J. Heagy (unpublished).
[40] J. M. Green, R. S. MacKay, F. Vivaldi, and M. J. Feigenbaum, Physica D **3**, 468 (1981).
[41] C. Jung (unpublished).
[42] L. Wiesenfeld, Phys. Lett. A **144**, 467 (1990).
[43] Zi-Min Lu, James F. Heagy, Michel Vallières, and Jian-Min Yuan, Phys. Rev. A **43** , 1118 (1991).